

# 1 Quantification of atmospheric nucleation and growth process 2 as a single source of aerosol particles in a city

3 Imre Salma, Veronika Varga, Zoltán Németh

4 Institute of Chemistry, Eötvös University, H-1518 Budapest, P.O. Box 32, Hungary

5 Correspondence to: Imre Salma (salma@chem.elte.hu)

6 **Abstract.** Effects of new aerosol particle formation (NPF) and particle diameter growth process as a single source on  
7 atmospheric particle number concentrations were evaluated and quantified on the basis of experimental data sets obtained from  
8 particle number size distribution measurements in the city centre and near-city background of Budapest for 5 years. Nucleation  
9 strength factors separately for a nucleation day ( $NSF_{NUC}$ ) and for a general day ( $NSF_{GEN}$ ) were derived for seasons and full  
10 years. The former characteristics represents the concentration increment of ultrafine (UF) particles specifically on nucleation  
11 days with respect to ~~accumulation-mode (regional background)-particle~~ concentration (particles with equivalent diameters of  
12 100–1000 nm;  $N_{100-1000}$ ) due solely to nucleation process. The latter factor expresses the contribution of nucleation to particle  
13 numbers on general days, thus it represents a longer time interval such as season or year. The nucleation source had the largest  
14 effect on the concentrations around noon and early afternoon as expected. During this time interval, it became the major source  
15 of particles in the near-city background. Nucleation increased the daily mean ~~particle number~~ concentrations on nucleation  
16 days by mean factors of 2.3 and 1.58 in the near-city background and city centre, respectively. Its effect was the largest in  
17 winter, which was explained with the substantially lower ~~background concentration~~  $N_{100-1000}$  levels on nucleation days than  
18 that on non-nucleation days. On an annual time scale, 37% of the UF particles were generated by nucleation in the near-city  
19 background, while NPF produced 13% of UF particles in the city centre. The differences among the annual mean values, and  
20 among the corresponding seasonal mean values were likely caused by the variability in controlling factors from year to year.  
21 The values obtained represent lower limits of the contributions. The shares determined imply that NPF is a non-negligible or  
22 substantial source of particles in near-city background environments and even in city centres, where the vehicular road  
23 emissions usually prevail. Atmospheric residence time of nucleation-mode particles was assessed by a decay curve analysis ~~of~~  
24  ~~$N_{6-25}$  concentrations in time~~, and a mean of 2:30 was obtained. The present study suggests that the health-related consequences  
25 of atmospheric NPF and growth process in cities should also be considered in addition to its urban climate implications.

## 26 1 Introduction

27 Large-scale modelling studies suggest that new aerosol particle formation (NPF) and consecutive particle diameter growth  
28 process in the atmosphere (Kulmala et al., 2004, 2013) is the dominant source of particle number concentrations on global  
29 scale (Spracklen et al., 2006; Reddington et al., 2011; Makkonen et al., 2012; Yu et al., 2015). In addition, up to approximately  
30 50% of all cloud condensation nuclei (CCN) can originate from NPF and growth (Spracklen et al., 2008; Merikanto et al.,  
31 2009), which relates the process to the climate system, and indicates its overall importance (Kerminen et al., 2012; Carslaw et  
32 al., 2013; Shen et al., 2017). New particle formation has also been proved to be common in large cities (Nieminen et al., 2017).  
33 Urban NPF can interact with and can be influenced by regional nucleation events at least under some geographic conditions,  
34 and can become part of a phenomenon with a much larger horizontal extension than the city (Salma et al., 2016b). At the same  
35 time, particle number concentrations in cities are strongly affected by high-temperature emission sources from different sectors  
36 (Paasonen et al. 2016) such as household and residential heating (e.g. Butt et al., 2016), industrial processes and power  
37 production (e.g. Xiao et al., 2015), and vehicular road traffic (e.g. Morawska et al., 2008). Their diurnal variation often show  
38 daily time-activity pattern of inhabitants (Dall'Osto et al., 2013). Relative contributions of primary and secondary particle  
39 sources – particularly in cities – change substantially in time and space (Pikridas et al., 2015; Posner and Pandis, 2015). Several

40 methods were proposed to distinguish the major production types of particles (e.g. Shi et al., 1999; Alam et al., 2003; Rodrigues  
41 and Cuevas, 2007; Qian et al., 2007; Park et al., 2008; Costabile et al., 2009; Brines et al., 2015). The share of NPF as a single  
42 source of ambient particle number concentrations specifically in cities remained, however, largely unknown despite the fact  
43 that there is often a spatial coincidence between the poorer air quality and population density (Samoli et al., 2016). Moreover,  
44 approximately 70–80% of total particles in cities belong to the ultrafine (UF) size range (with an equivalent diameter <100  
45 nm; Putaud et al., 2010), and their inhalation can represent an excess health risk relative to coarse or fine particles with the  
46 same or similar chemical composition (Oberdörster et al., 2005; Braakhuis et al., 2014). An estimate on the relative contribution  
47 of primary and secondary formation processes is also required for efficient action plans to improve the air quality in cities. It  
48 is worth noting that indirect climate effects (due to CCN) become important for particles with diameters >50–100 nm, while  
49 the excess health effects are linked with diameters <100 nm.

50

51 Nucleation strength factor (NSF) was introduced to assess the contribution of NPF to UF particle number concentrations  
52 relative to accumulation-mode (regional background) concentration (particles with diameters of 100–1000 nm;  $N_{100-1000}$ ) with  
53 respect to all other sources (Salma et al., 2014). The results derived from this approach correspond to the mode-segregated  
54 secondary particle load. By now, atmospheric concentration data sets are available for multiple years to study the applicability,  
55 and-behaviour and interpretation of the NSF in detail. The major advantage of this quantification approach is that it only  
56 requires experimental data that can be readily derived from ordinary NPF (size distributions) measurements. The main  
57 objectives of this paper are to quantify and discuss the contribution of NPF events to ambient particle number concentrations  
58 in near-city and central urban environments of a Central European city considering five-year long data sets, to investigate and  
59 explain the meaning and further details of the NSF, and to interpret the consequences achieved for the urban air and air quality.

## 60 2 Methods

### 61 2.1 Experimental

62 The measurements were performed in Budapest, Hungary. Its population is approximately 2.5 million in the metropolitan area.  
63 The major pollution sources in terms of particle number include vehicular road traffic, residential heating and household  
64 burning activities. Contributions of passenger cars and buses to the vehicle fleet registered in Budapest and Pest County are  
65 87% and 0.46%, respectively (OKJ, 2015). Diesel-powered vehicles shared 19% and 97% of the national passenger car and  
66 bus fleets, respectively. Wintertime median concentrations of particulate matter (PM) mass, elemental carbon (EC) and organic  
67 carbon (OC) in the  $PM_{2.5}$  size fraction were 25, 0.97 and 4.9  $\mu\text{g m}^{-3}$ , respectively in the related time interval (Salma et al.,  
68 2017). The mean contributions of EC and organic matter (OM, with an OM/OC mass conversion factor of 1.6) to the  $PM_{2.5}$   
69 mass and standard deviation (SD) were  $4.8 \pm 2.1\%$  and  $37 \pm 10\%$ , respectively, while the contribution of  $(\text{NH}_4)_2\text{SO}_4$  and  $\text{NH}_4\text{NO}_3$   
70 derived from an earlier study in spring were 24% and 3%, respectively. The contributions of EC and OC from fossil fuel  
71 combustion to the total carbon contained in particles (TC=OC+EC) were 11.0% and 25%, respectively, and EC and OC from  
72 biomass burning were responsible for 5.8% and 34%, respectively of the TC, while the OC from biogenic sources made up  
73 24% of the TC.

74

75 Two urban sites were involved in the study. Most measurements were performed at the Budapest platform for Aerosol Research  
76 and Training (BpART) facility (N 47° 28' 29.9", E 19° 3' 44.6", 115 m above mean sea level (a.s.l.) of the Eötvös University  
77 (Salma et al., 2016a). The sampling inlets were set up at heights between 12 and 13 m above the street level. The location  
78 represents a well-mixed, average atmospheric environment for the city centre. The other location was situated at the NW border  
79 of Budapest in a wooded area of the Konkoly Astronomical Observatory of the Hungarian Academy of Sciences (N 47° 30'  
80 00.0", E 18° 57' 46.8", 478 m a.s.l.). It represents the air masses entering the city since the prevailing wind direction in the area

81 is NW. The experimental data obtained for five full-year long time intervals, i.e. from 03–11–2008 to 02–11–2009, from 19–  
 82 01–2012 to 18–01–2013, from 13–11–2013 to 12–11–2014, from 13–11–2014 to 12–11–2015 and from 13–11–2015 to 12–  
 83 11–2016 were considered in the present study. Local time (UTC+1 and daylight saving time, UTC+2) was chosen as the time  
 84 scale because the daily routine activities of the inhabitants in the city were primarily considered.

85

86 The key measuring instrument was a flow-switching type differential mobility particle sizer (DMPS; Salma et al., 2011). Its  
 87 main components include a Ni-60 radioactive bipolar charger, a Nafion semi-permeable membrane dryer, a 28-cm long  
 88 Vienna-type differential mobility analyser and a butanol-based condensation particle counter (TSI, model 3775). The system  
 89 operates in an electrical mobility diameter range from 6 to 1000 nm in the dry state of particles (with a relative humidity  
 90 RH<30%) in 30 channels with a time resolution of approximately 8 or 10 min at two sets of flows. The sample flow rate is 2.0  
 91 L min<sup>-1</sup> in high-flow mode, and 0.31 L min<sup>-1</sup> in low-flow mode with sheath air flow rates 10 times larger than for the sample  
 92 flows. The DMPS measurements were performed according to the international technical standard (Wiedensohler et al., 2012).  
 93 The DMPS data for the 1-year long time intervals in 2008–2009, 2012–2013, 2013–2014, 2014–2015 and 2015–2016 were  
 94 available in 95%, 95%, 99%, 95% and 73% of the total number of days, respectively. Meteorological data were recorded by  
 95 an on-site meteorological station (Salma et al., 2016a). Standardised meteorological measurements of air temperature (*T*), RH,  
 96 wind speed and wind direction were recorded with a time resolution of 10 min. The coverage of the meteorological data was  
 97 >80% in each year.

## 98 2.2 Data treatment

99 The overall treatment of the measured DMPS data was performed according to the procedure protocol by Kulmala et al. (2012).  
 100 The inverted DMPS data were utilised to generate particle number size distribution surface plots showing jointly the variation  
 101 in particle diameter and particle number concentration density in time. Identification and classification of NPF and growth  
 102 events was accomplished from the surface plots by using the algorithm similar to that of Dal Maso et al. (2005) on a day-to-  
 103 day basis into the following main classes: NPF event days, non-event days, days with undefined character, and days with  
 104 missing data (for more than 4 h in the midday). Frequency of events was determined as the ratio of the number of event days  
 105 to the total number of relevant (i.e. all–missing) days. Particle number concentrations in the diameter ranges from 6 to 1000  
 106 nm ( $N_{6-1000}$ ), from 6 to 100 nm ( $N_{6-100}$ ), from 6 to 25 nm ( $N_{6-25}$ ) and from 100 to 1000 nm ( $N_{100-1000}$ ) were calculated from the  
 107 DMPS data. The major portion of the  $N_{6-100}$  concentration (i.e. in the Aitken mode **plus sporadically the nucleation mode**) is  
 108 essentially related to local source processes due to the limited atmospheric residence time (typically <10<sup>1</sup> h) of these particles,  
 109 while the  $N_{100-1000}$  (**regional background** concentration **associated** mainly with the accumulation mode) expresses larger  
 110 **(background)** spatial and time scales because of much longer residence times (up to 10<sup>1</sup> d; Salma et al., 2011). To obtain mean  
 111 diurnal variation of the concentrations and further properties derived from them (see later), the exact recording times belonging  
 112 to the individual concentrations were rounded off to 5 min (in case of the time resolution of ca. 8 min) or 10 min (in case of  
 113 the time resolution of ca. 10 min) time scale. These data were averaged by the time of day separately for nucleation and non-  
 114 nucleation days. Finally, the averaging was also performed separately for different seasons, hence for spring (March-May),  
 115 summer (June-August), autumn (September-November) and winter (December-February), and for the measurement year.

116

117 Two types of NSF (Salma et al., 2014) were derived in the present study by considering different conditions. The quantity:

$$118 \text{NSF}_{\text{NUC}} = \frac{\left( \frac{N_{6-100}}{N_{100-1000}} \right)_{\text{nucleationdays}}}{\left( \frac{N_{6-100}}{N_{100-1000}} \right)_{\text{non-nucleationdays}}} \quad (1)$$

119 considers the  $N_{6-100}/N_{100-1000}$  concentration ratios for nucleation days only. The numerator expresses the increase in  $N_{6-100}$   
 120 relative to the ~~background concentration~~  $N_{100-1000}$  caused by all source sources. The denominator represents the same property  
 121 due to all sources except for NPF. Hence, the  $NSF_{NUC}$  accounts for the ~~concentration increment in background particle~~  
 122 ~~concentration~~ on a nucleation day exclusively caused by NPF. It was implicitly assumed that the major emission and formation  
 123 processes of UF particles except for NPF are uniformly present on both nucleation and non-nucleation days. It seems to be a  
 124 reasonable condition for time intervals of several months, although the number of nucleation days during a time interval  
 125 actually plays a more determining role than the length of the time interval. Winter, when the occurrence frequency shows the  
 126 minimum (see Table 1), appears to be the most restrictive or critical season. The effect of the non-uniformly present sources  
 127 is indicated by unusually larger scatter in the diurnal data points (see Sect. 3.2). It was also presumed that the production of  
 128 particles larger than 100 nm was much smaller than the concentration of UF particles. This is ordinarily realised in cities, and  
 129 can be justified from the contributions of UF particles to the total particle number (Putaud et al., 2010; Németh et al., 2017).

130  
 131 The other type of NSF was calculated for all days in the numerator, thus:

$$132 \quad NSF_{GEN} = \frac{\left( \frac{N_{6-100}}{N_{100-1000}} \right)_{\text{all days}}}{\left( \frac{N_{6-100}}{N_{100-1000}} \right)_{\text{non-nucleationdays}}} \quad (2)$$

133 It expresses the overall contribution of NPF to ~~particle numbers of  $N_{100-1000}$  background concentration~~ on longer time span, so  
 134 in general. Since there are usually more non-nucleation days than nucleation days in a time interval of month or more  
 135 (Nieminen et al., 2017), the assumptions for  $NSF_{GEN}$  are met easier than for  $NSF_{NUC}$ . The  $NSF_{NUC}$  characterises an ordinary  
 136 nucleation day within e.g. a season, while the  $NSF_{GEN}$  quantifies the overall effect of NPF and growth on the atmospheric  
 137 concentrations on a regular/average day over e.g. a season or year. ~~The former is always larger than the latter due to their~~  
 138 ~~definition. They can be calculated for seasons or years. Despite their relatively simple mathematical definition, the exact~~  
 139 ~~meaning and rigorous interpretation of the  $NSF_{NUC}$  and  $NSF_{GEN}$  are complex, and they should be approach with care in~~  
 140 ~~particular, as far as the assumptions for their utilisation are concerned.~~ If 1)  $NSF \approx 1$  then the relative contribution of nucleation  
 141 to particle number concentrations with respect to other sources is negligible, 2)  $1 < NSF < 2$  then its relative contribution as a  
 142 single source is considerable, and 3)  $NSF > 2$  then the contribution of nucleation itself to particle number concentrations is  
 143 larger than of any other source sectors together. ~~The interpretation regarding the limiting values is valid for both types of NSF.~~  
 144 Since the major phase of NPF and growth process takes place in most cases in one day, it is advantageous to express NSFs as  
 145 daily mean values. The data for the undefined days were not taken into account for the present evaluation.

### 146 3 Results and discussion

147 Number of nucleation days for different seasons in each measurement year are summarised in Table 1. It is seen that the NPF  
 148 frequency has an obvious seasonal variation. This can be obtained from its monthly dependency which exhibits an absolute  
 149 and local minimum in January and August, respectively, and an absolute and local maximum in March or April, and September,  
 150 respectively (Salma et al., 2016b). The seasonal variation of the nucleation frequency fits into the second group of the  
 151 measurement sites - ~~which is characterised by the highest number of nucleation events in spring and the lowest in winter, with~~  
 152 ~~relatively high total number of events reported by~~ (Manninen et al., 2010).

153

154  
155

**Table 1.** Number of nucleation days for seasons in the near-city background (in 2012–2013) and in the city centre (in 2008–2009, 2013–2014, 2014–2015 and 2015–2016) during 1-year long time intervals.

Environment	Time interval	Spring	Summer	Autumn	Winter
Background	2012–2013	35	20	24	17
Centre	2008–2009	34	21	22	6
Centre	2013–2014	28	20	13	11
Centre	2014–2015	41	19	14	7
Centre	2015–2016	15	9*	5*	6

156  
157

\* Low data coverage. See Sect. 2.1.

158

### 3.1 Seasonal atmospheric concentrations

159

Particle number concentrations in the related size fractions for different seasons in each measurement year are summarised in

160

Table 2 for an overview.

161

**Table 2.** Median atmospheric concentration of particles with a diameter from 6 to 100 nm ( $N_{6-100}$ ) and from 100 to 1000 nm ( $N_{100-1000}$ ) in units of  $10^3 \text{ cm}^{-3}$  separately on nucleation (Nuc) days and non-nucleation (Nonuc) days for seasons in the near-city background (in 2012–2013) and in the city centre (in 2008–2009, 2013–2014, 2014–2015 and 2015–2016) during 1-year long time intervals. Mean ratios of median concentrations on nucleation days to that on non-nucleation days with standard deviation (SD) for the size fraction are also indicated.

162

163

164

Urban environment			Near-city backgr.		City centre				
Time interval	Size fraction	Day type	2012–2013	Ratio	2008–2009	2013–2014	2014–2015	2015–2016	Ratio $\pm$ SD
Spring	$N_{6-100}$	Nuc	4.8	1.72	11.2	9.7	10.0	8.6	1.37
	$N_{6-100}$	Nonuc	2.8		8.9	7.2	7.1	5.9	$\pm 0.09$
	$N_{100-1000}$	Nuc	1.56	1.03	2.0	2.5	2.6	1.56	0.99
	$N_{100-1000}$	Nonuc	1.51		2.2	2.7	2.5	1.5	$\pm 0.07$
Summer	$N_{6-100}$	Nuc	4.0	1.37	10.3	8.0	8.6	6.9*	1.17
	$N_{6-100}$	Nonuc	2.9		8.9	7.5	6.5	6.2*	$\pm 0.11$
	$N_{100-1000}$	Nuc	1.27	0.89	1.36	2.0	2.5	1.40*	0.92
	$N_{100-1000}$	Nonuc	1.42		1.72	2.4	2.4	1.37*	$\pm 0.13$
Autumn	$N_{6-100}$	Nuc	4.3	1.29	14.0	11.9	12.6	5.2*	1.41
	$N_{6-100}$	Nonuc	3.3		10.4	8.5	8.4	5.1*	$\pm 0.08$
	$N_{100-1000}$	Nuc	1.67	0.74	2.0	3.4	2.7	1.6*	0.87
	$N_{100-1000}$	Nonuc	2.3		2.4	3.9	3.3	1.7*	$\pm 0.06$
Winter	$N_{6-100}$	Nuc	3.9	1.10	6.9	10.5	5.6	7.7	0.87
	$N_{6-100}$	Nonuc	3.6		12.5	9.2	7.8	7.4	$\pm 0.28$
	$N_{100-1000}$	Nuc	1.12	0.38	1.02	3.7	1.65	1.4	0.54
	$N_{100-1000}$	Nonuc	2.9		3.0	4.5	3.8	2.7	$\pm 0.22$

165

\* Low data coverage. See Sect. 2.1.

166

167

Data coverage for summer and autumn in 2015–2016 were low, and therefore, the corresponding concentration ratios were

168

excluded from the averaging for the mean ratios. It can be seen that the  $N_{6-100}$  were ordinarily larger on nucleation days than

169

on non-nucleation days. This is most likely a direct effect of nucleation. At the same time, the  $N_{100-1000}$  usually showed a

170

constant level within approximately 10% except for winters and some autumns. The  $N_{100-1000}$  background concentrations on

171

nucleation days were, however, smaller (by factors of 0.4–0.5) than for non-nucleation days, particularly in winter. The

172

differences are further discussed and explained in Sect. 3.2.

173

### 3.2 Concentration increment on nucleation days

174

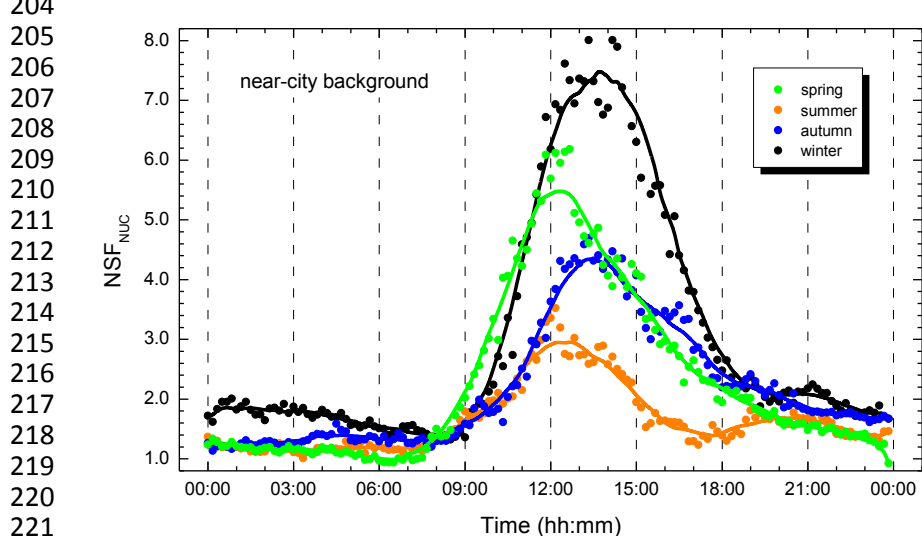
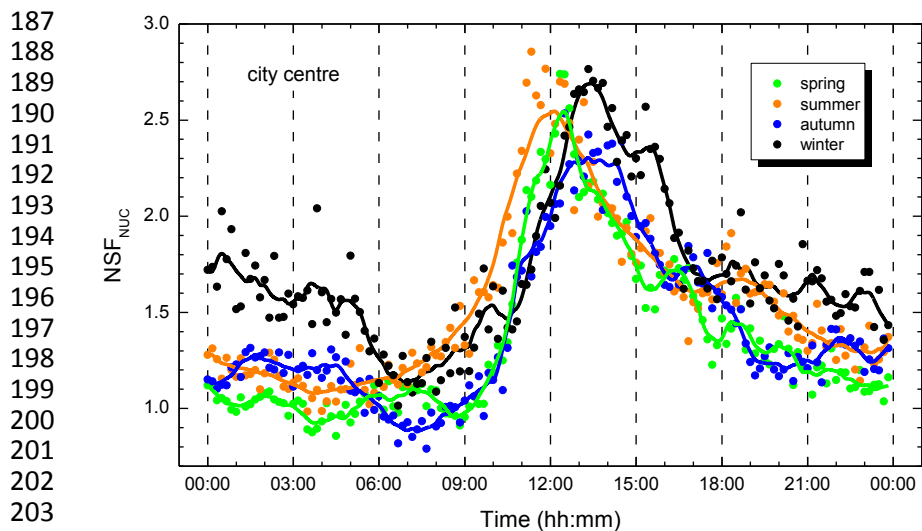
Diurnal variation of the concentration increment due to NPF on nucleation days (i.e. of  $NSF_{Nuc}$ ) for the city centre and near-

175

city background separately for different seasons are shown in Fig. 1 as representative examples. The curves exhibited a single

176 peak around noon with a longer tail on the decreasing side. The exact location of the peak is also influenced by setting the  
 177 local daylight saving time in spring and autumn. The baseline of some peaks from 0:00 to 7:00 deviated systematically and  
 178 substantially from unity although no nocturnal nucleation has been observed in Budapest. The mean values of this baseline in  
 179 the city centre for spring, summer, autumn and winter (Fig. 1 upper panel) were 1.02, 1.15, 1.15 and 1.55, respectively, while  
 180 they were 1.11, 1.18, 1.31 and 1.72, respectively in the near-city background (Fig. 1 lower panel). The elevated line can be  
 181 explained by the fact that particle growth process could be traced till the late morning of the next day in several occasions,  
 182 thus the NPF influenced the  $N_{6-100}$  concentrations over the next morning. This affected the baseline if a non-nucleation day  
 183 followed a nucleation day, and particularly, in the seasons when NPF events occur well separated from each other in time,  
 184 which is typical for winter. The elevated baseline is a real effect of the NPF, and **it should be definitely included in deriving  
 185 the mean  $NSF_{NUC}$ -consideration in the averaging is justified.**

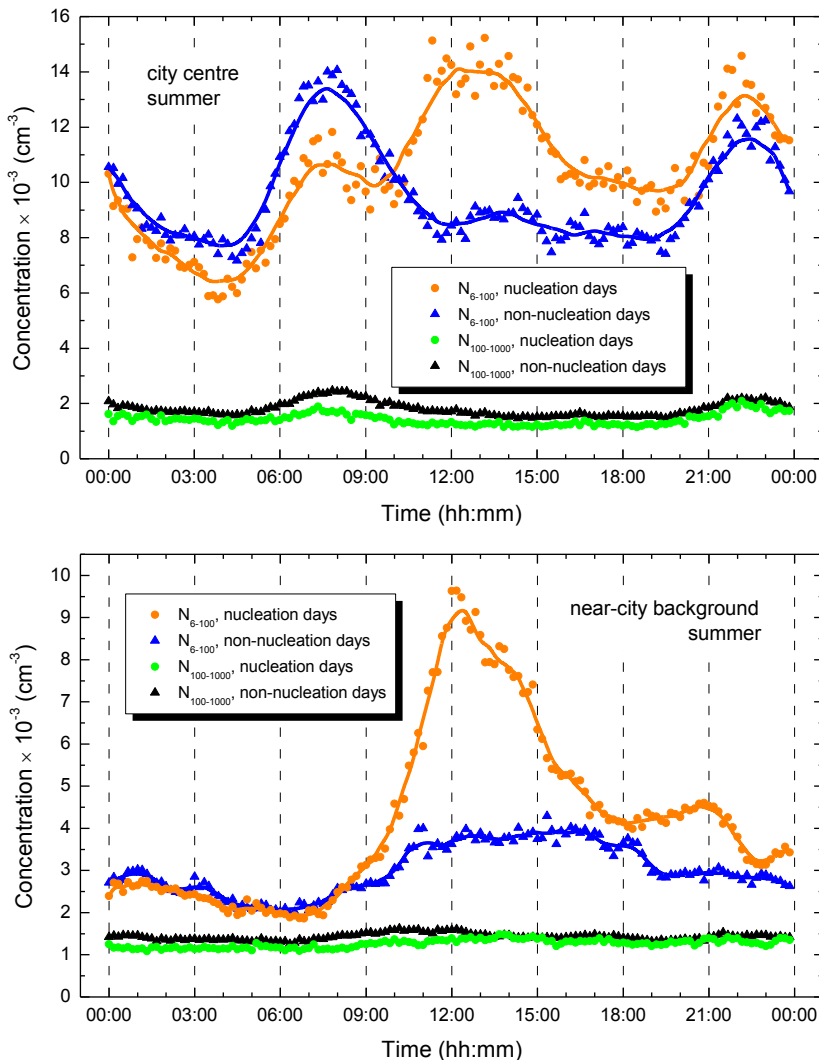
186



223 **Figure 1.** Diurnal variation of concentration increment on a nucleation day ( $NSF_{NUC}$ ) due to new particle formation and growth for the city  
 224 centre in 2008–2009 (upper panel) and in the near-city background in 2012–2013 (lower panel) separately for seasons. The solid lines  
 225 represent 1-h smoothing to the data.  
 226

227 It was also observed in all years that the concentration increment on nucleation days due to NPF (i.e.  $NSF_{GEN}$ ) was the largest  
 228 for winter. This evidently showed up for the near-city background. It was followed by the other seasons which had similar  
 229 importance to each other in the city centre, or which were ordered as spring, autumn and summer in the near-city background.  
 230 To investigate these findings more closely, diurnal variation of the related particle number concentrations were derived and  
 231 evaluated. Diurnal variation of the concentrations for summer and winter are shown in Figs. 2 and 3, respectively for the city

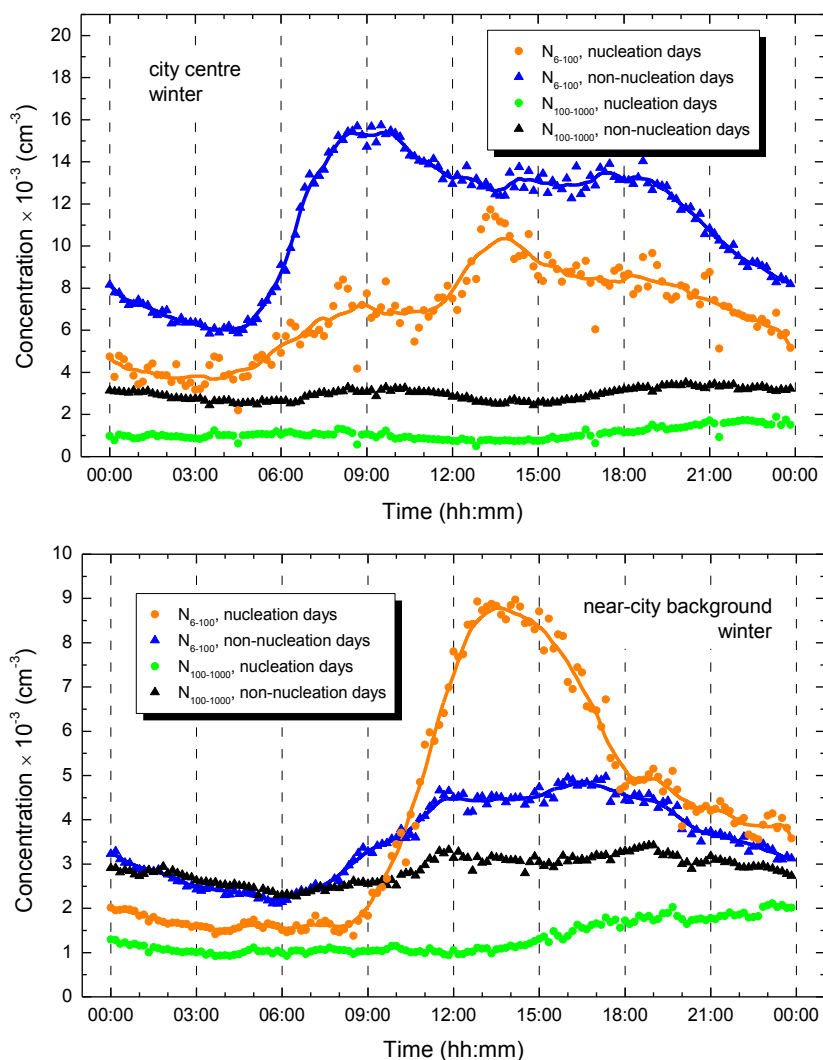
232 centre and near-city background. The dependencies in the city centre for the spring, autumn and other summer seasons are  
 233 similar to Fig. 2 upper panel, while the corresponding seasonal curves for the near-city background resemble Fig. 2 lower  
 234 panel. The diurnal patterns represented by Fig. 2 are coherent with the previous ideas on the NPF and growth events in the  
 235 Budapest area (Salma et al., 2014, 2016b; Németh et al., 2017). They also confirm the basic assumptions of the NSF<sub>NUC</sub>  
 236 definition on the source intensities at both location types. The comparison of the  $N_{6-100}$  curves for nucleation days and non-  
 237 nucleation days already emphasizes the importance of NPF, and indicates that the phenomenon has larger relative effect in the  
 238 near-city background than in the central urban parts - as it is expected. The late evening peak can be likely related to the  
 239 combined effect of burning activities at residences and homes, of local meteorology, and they are also influenced by the daily  
 240 cycling of the boundary layer mixing height and mixing intensity. As far as the  $N_{6-100}$  between 06:00 and 09:00 is concerned,  
 241 its higher level on non-nucleation days with respect to nucleation days is related to higher pre-existing aerosol concentration  
 242 level, and thus, to larger condensation sink values, which hinder NPF. The particle number concentrations for the background  
 243 aerosol ( $N_{100-1000}$ ) curves appear close to each other within a relative uncertainty of 10–20%, which implies that the  
 244 accumulation-mode background concentrations affect the NPF occurrence and formation rate in a limited manner in these  
 245 seasons.



282 **Figure 2.** Diurnal variation of particle number concentrations in summer for the diameter ranges from 6 to 100 nm ( $N_{6-100}$ ) and from 100 to  
 283 1000 nm ( $N_{100-1000}$ ) in the city centre in 2008–2009 (upper panel) and in the near-city background in 2012–2013 (lower panel) separately for  
 284 nucleation days and non-nucleation days. The solid lines represent 1-h smoothing to the data.

286 For winter, it is seen, however, that the  $N_{100-1000}$  background concentrations were substantially different for the nucleation and  
 287 non-nucleation days (Fig. 3). The mean non-nucleation/nucleation  $N_{100-1000}$  ratios for the city centre (in 2008–2009) and near-

288 city background were 2.8 and 2.3, respectively. This implies that the NPF events preferably took place on those days when the  
 289 particle number concentrations were generally smaller. It is understandable if we consider that the basic preconditions of NPF  
 290 events are realised by competing source and sink for condensing vapours. The source strength in winter has a decreased  
 291 tendency due to lower solar radiation intensities and less (biogenic) precursor gases in the air. **There is indirect evidence that**  
 292 **biogenic emissions contribute to the early stage of the growth process, and likely, to the nucleation itself as well (Salma et al.,**  
 293 **2016b).** Nevertheless, nucleation can occur at these small source terms if the (condensation and scavenging) sink - which is  
 294 related to the concentration of pre-existing particles - is even smaller. This explains the differences in the  $N_{100-1000}$ **background**  
 295 **concentrations** on nucleation and non-nucleation days. Larger concentration increments (higher  $NSF_{NUC}$ , Fig. 3) for winter  
 296 were simply caused by systematically smaller  $N_{100-1000}$ **background concentrations** on nucleation days. In addition, the  
 297 fluctuation in **this concentration**  $N_{100-1000}$  for nucleation days in winter of the other years was sometimes larger than that  
 298 shown in Fig. 3. This observation raises the question of **which is** the smallest number of NPF events in a time interval (e.g.  
 299 season) that **is can be considered** sufficient for obtaining representative **mean diurnal concentration data for calculating the**  
 300  $NSF_{NUC}$ . A few NPF events during winters (see Table 1) may not be fully satisfactory for this purpose. **The longer time intervals**  
 301 **needed do not detract from the value of the quantification, because the health and environmental effects of NPF are important**  
 302 **mostly on longer time scales.**



341 **Figure 3.** Diurnal variation of particle number concentrations in winter for the diameter ranges from 6 to 100 nm ( $N_{6-100}$ ) and from 100 to  
 342 1000 nm ( $N_{100-1000}$ ) in the city centre in 2008–2009 (upper panel) and in the near-city background in 2012–2013 (lower panel) separately for  
 343 nucleation days and non-nucleation days. The solid lines represent 1-h smoothing to the data.  
 344



345 Seasonal and annual mean concentration increments on a nucleation day (hence the daily mean  $NSF_{NUC}$  values) for different  
 346 years are summarised in Table 3. Nucleation as a single source increased the daily particle number concentrations by factors  
 347 of 2.3 and 1.58 in the near-city background and city centre, respectively on an annual time scale. The differences among the  
 348 annual mean values, and among the corresponding seasonal mean values were likely caused by the variability of controlling  
 349 parameters from a year to year. As far as the seasonal variation is concerned, it is noted that the formation rate for particles  
 350 with a diameter of 6 nm ( $J_6$ ) showed only limited seasonal dependency in Budapest (Salma et al., 2011), which also contributed  
 351 to similar mean increments for spring, summer and autumn.

352 **Table 3.** Seasonal and annual mean increments of **background-concentration**  $N_{100-1000}$  due to nucleation on a nucleation day (nucleation  
 353 strength factor  $NSF_{NUC}$ ) in the near-city background (in 2012–2013) and in the city centre (in 2008–2009, 2013–2014, 2014–2015 and 2015–  
 354 2016) during 1-year long time intervals.

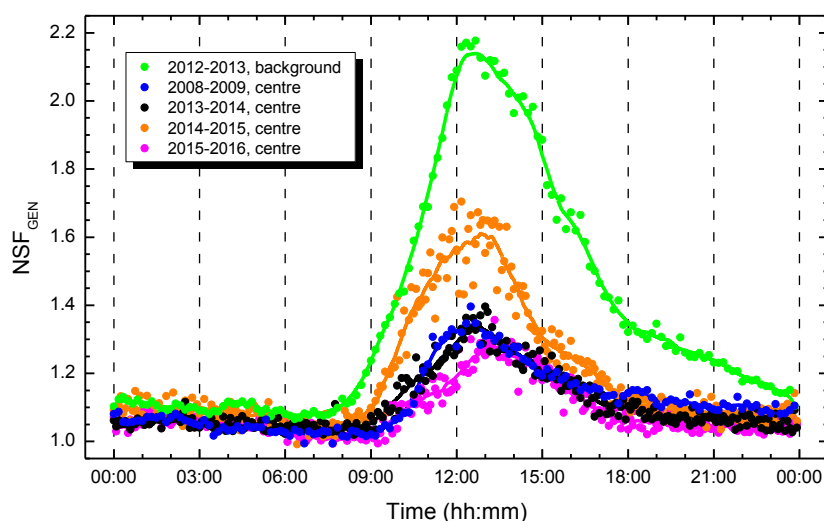
Urban environment	Time interval	$NSF_{NUC}$				
		Spring	Summer	Autumn	Winter	Year
Background	2012–2013	2.3	1.66	2.2	3.0	2.3
Centre	2008–2009	1.36	1.55	1.42	1.71	1.49
Centre	2013–2014	1.31	1.33	1.36	1.56	1.44
Centre	2014–2015	1.50	1.34	1.83	2.8	1.73
Centre	2015–2016	1.54	1.26	1.46	2.4	1.64

355

### 356 3.3 Contribution of nucleation to particle number concentrations

357 Diurnal variation of  $NSF_{GEN}$  is shown in Fig. 4. The curves exhibited a single peak with a maximum around noon and a longer  
 358 tail in the early afternoon. The maximum values in the city centre represented concentration contributions from 30% to 60%  
 359 due to nucleation for a limited time interval. The curve for the near-city background was the largest, as expected, and it even  
 360 exceeded the value of 2 around noon for approximately 3 h. This all means that nucleation has an important contribution to  
 361 UF particles during the midday in the city centre, while it even becomes the dominant source of particles directly after midday  
 362 in the near-city background.

363



364  
 365  
 366  
 367  
 368  
 369  
 370  
 371  
 372  
 373  
 374  
 375  
 376  
 377  
 378  
 379  
 380  
 381  
 382 **Figure 4.** Diurnal variation of NPF contribution to particle number concentrations ( $NSF_{GEN}$ ) in the near-city background (in 2012–2013)  
 383 and in the city centre (in 2008–2009, 2013–2014, 2014–2015 and 2015–2016) during 1-year long time intervals. The solid lines represent 1-  
 384 h smoothing to the data.

385

386 The importance of nucleation was also demonstrated for different seasons and years by the mean  $NSF_{GEN}$  values which are  
 387 summarised in Table 4. In general, 37% of UF particles (more precisely of particle number increase) were produced by

388 nucleation as a single source in the near-city background. In the city centre, it generated 13% of UF particles. These values  
 389 can be considered as lower limits since a considerable part of  $N_{100-1000}$  background particles can be also produced by NPF from  
 390 previous days. Nevertheless, the proposed method is capable of quantifies the relevance of particles from NPF relative to other  
 391 sources for the first time, which is an unambiguous and important step forward in urban atmospheric studies. The differences  
 392 among the annual mean values, and among the corresponding seasonal mean values were likely caused by the year-to-year  
 393 variability similarly to the concentration increments on nucleation days ( $NSF_{NUC}$ ). It is informative to compare the contribution  
 394 values to the global share of various source sectors in primary UF particle number emission to have an idea on the relative  
 395 extent of our results. It is stressed that our and the literature data are related to very different types of particles, nevertheless,  
 396 some analogy can be found in the relative importance of the sources and source processes. Road transport, power production  
 397 and residential combustion are the first three largest contributors to primary UF particles with the shares of 40%, 20% and  
 398 17%, respectively (Paasonen et al., 2016). The actual contributions can vary in different parts of the world and with economic  
 399 development.

400  
 401 The effects of particles generated by NPF and growth in increased concentrations on human health and the environment are  
 402 also influenced by the time interval for which the particles remain in the air. Nucleation-mode particles are primarily removed  
 403 by coagulation with larger particles, agglomeration, diffusion and turbulent losses, scavenging and various aging processes.  
 404 We showed in Sect. 3.2 and it can be also proved directly from the measured data that it is the NPF events that usually produce  
 405 the  $N_{6-25}$  concentrations in an overwhelming extent (the  $N_{6-25}$  is increased by 1–2 orders of magnitude) in a relatively short  
 406 time interval. The continual concentration decrease in time for several hours after the event can be utilised to assess the general  
 407 atmospheric residence time of nucleation-mode particles. The decrease of this concentration after a nucleation burst could be  
 408 approximated by an exponential function (first order kinetics). By a decay curve analysis of 15 selected NPF and particle  
 409 diameter growth cases, the residence times were estimated from the slope of the concentrations  $N_{6-25}$  in a natural logarithmic  
 410 scale versus time. The residence time of nucleated particles varied from 1:30 to 4:15 with a mean and SD of  $2:30 \pm 1:00$ . This  
 411 suggests that the nucleation-mode particles (or in other words the nucleated particles in their very small sizes, or atmospheric  
 412 nanoparticles) likely have limited health effects due to their relatively short existence in the air.

413 **Table 4.** Seasonal and annual mean contributions of nucleation to  $N_{100-1000}$  background concentration (nucleation strength factor  $NSF_{GEN}$ )  
 414 in the near-city background (in 2012–2013) and in the city centre (in 2008–2009, 2013–2014, 2014–2015 and 2015–2016) during 1-year  
 415 long time intervals.

Urban environment	Time interval	$NSF_{GEN}$				
		Spring	Summer	Autumn	Winter	Year
Background	2012–2013	1.51	1.18	1.31	1.40	1.37
Centre	2008–2009	1.12	1.15	1.10	1.05	1.12
Centre	2013–2014	1.11	1.07	1.08	1.11	1.11
Centre	2014–2015	1.22	1.08	1.14	1.16	1.19
Centre	2015–2016	1.09	1.06	1.03	1.09	1.09

#### 416 4 Conclusions

417 We showed in the present study that NPF and particle diameter growth process as a single source represents a considerable  
 418 contribution to UF particles in a Central European city with respect to all other emission sources including vehicular road  
 419 traffic. Nucleation was a major process that produced UF particles at noon and in the early afternoon, and its relative  
 420 contribution was comparable to other production sources during this time period even in the city centre. Relative importance  
 421 of nucleation as a source of particles decreased with anthropogenic influence. The NSF<sub>s</sub> were defined by utilising  $N_{6-100}$  and  
 422  $N_{100-1000}$  concentrations. There are several sensible and practical reasons for selecting these specific size fractions although

423 other dividing values are also imaginable. The quantifications in the present study are, therefore, subjected to certain inherent  
424 uncertainty. Considering that the modes of the particle number size distribution are usually shifted to smaller diameters in  
425 cities with respect to rural or remote areas, it seems realistic that these size fractions represent well the particles of urban (local)  
426 origin and the aged particles (which characterize larger spatial or urban background area), respectively. The study also suggests  
427 that particles from NPF events in cities are relevant not only for their effects on urban climate but because of their health risk  
428 to inhabitants. At the same time, it should also be mentioned that ambient atmospheric aerosol which ordinary persists in the  
429 air of cities contains particles in the largest abundance with a diameter between approximately 25 and 150 nm. **Atmospheric**  
430 **aerosol system containing** smaller particles **is** thermodynamically not stable, and most of **these particles** are removed from the  
431 air during relatively short time intervals. The exposures to freshly nucleated particles ( $d < 25$  nm) or ambient nanoparticles  
432 ( $d < 10$  nm) are usually limited to several hours after the onset of the NPF.

433  
434 Regulations of aerosol emissions and atmospheric concentrations are usually based on PM mass. The changes or reductions in  
435 anthropogenic aerosol load are ordinary assessed by assuming similar relative tendencies in particle mass and particle number  
436 concentrations. This generalisation may yield to tentative conclusions. According to current legislation scenarios, particle  
437 number emissions are expected to decrease in most part of the world by 2030 mainly due to spreading the diesel particulate  
438 filters (DPF) in cars and due to diesel fuels with ultralow sulphur content. In effect, this may imply that the relative share of  
439 NPF in the particle number production is expected to increase above the levels estimated in the present study. By demonstrating  
440 the relevance of NPF as an important single source of UF particles, we also raise the question of an international enhanced  
441 particle mass and particle number inventory with precursor gas data that potentially includes the NPF and growth process as a  
442 separate sector among the source types.

## 443 **5 Data availability**

444 The relevant observational data used in this paper are available on request from the corresponding author or at the website of  
445 the Budapest platform for Aerosol Research and Training (<http://salma.web.elte.hu/BpArt>).

446 *Competing interests.* The authors declare that they have no conflict of interest.

447 *Acknowledgement.* Financial supports by the National Research, Development and Innovation Office of Hungary (contract  
448 K116788) is appreciated.

## 449 **References**

- 450 Alam, A., Shi, J. P., and Harrison, R. M.: Observation of new particle formation in urban air, *J. Geophys. Res.*, 108, 4093–  
451 4107, 2003.
- 452 Braakhuis, H. M., Park, M. V., Gosens, I., De Jong, W. H., and Cassee, F. R.: Physicochemical characteristics of  
453 nanomaterials that affect pulmonary inflammation, *Part. Fibre Toxicol.*, 11:18, doi: 10.1186/1743-8977-11-18, 2014.
- 454 Brines, M., Dall'Osto, M., Beddows, D. C. S., Harrison, R. M., Gómez-Moreno, F., Núñez, L., Artíñano, B., Costabile, F.,  
455 Gobbi, G. P., Salimi, F., Morawska, L., Sioutas, C., and Querol, X.: Traffic and nucleation events as main sources of  
456 ultrafine particles in high-insolation developed world cities, *Atmos. Chem. Phys.*, 15, 5929–5945, 2015.
- 457 Butt, E. W., Rap, A., Schmidt, A., Scott, C. E., Pringle, K. J., Reddington, C. L., Richards, N. A. D., Woodhouse, M. T.,  
458 Ramirez-Villegas, J., Yang, H., Vakkari, V., Stone, E. A., Rupakheti, M., S. Praveen, P., G. van Zyl, P., P. Beukes, J.,  
459 Josipovic, M., Mitchell, E. J. S., Sallu, S. M., Forster, P. M., and Spracklen, D. V.: The impact of residential combustion  
460 emissions on atmospheric aerosol, human health, and climate, *Atmos. Chem. Phys.*, 16, 873–905, 2016.

461 Carslaw, K. S., Lee, L. A., Reddington, C. L., Pringle, K. J., Rap, A., Forster, P. M., Mann, G. W., Spracklen, D. V.,  
462 Woodhouse, M. T., Regayre, L. A., and Pierce, J. R: Large contribution of natural aerosols to uncertainty in indirect  
463 forcing, *Nature*, 503, 67–71, 2013.

464 Carslaw, K. S., Lee, L. A., Reddington, C. L., Pringle, K. J., Rap, A., Forster, P. M., Mann, G. W., Spracklen, D. V.,  
465 Woodhouse, M. T., Regayre, L. A., and Pierce, J. R: Large contribution of natural aerosols to uncertainty in indirect  
466 forcing, *Nature*, 503, 67–71, 2013.

467 Costabile, F., Birmili, W., Klose, S., Tuch, T., Wehner, B., Wiedensohler, A., Franck, U., König, K., and Sonntag, A.:  
468 Spatio-temporal variability and principal components of the particle number size distribution in an urban atmosphere,  
469 *Atmos. Chem. Phys.*, 9, 3163–3195, 2009.

470 Dal Maso, M., Kulmala, M., Riipinen, I., Wagner, R., Hussein, T., Aalto, P. P., and Lehtinen, K. E. J.: Formation and growth  
471 of fresh atmospheric aerosols: eight years of aerosol size distribution data from SMEAR II, Hyytiälä, Finland, *Boreal  
472 Environ. Res.*, 10, 323–336, 2005.

473 Dall'Osto, M., Querol, X., Alastuey, A., O'Dowd, C., Harrison, R. M., Wenger, J., and Gómez-Moreno, F. J.: On the spatial  
474 distribution and evolution of ultrafine particles in Barcelona, *Atmos. Chem. Phys.*, 13, 741–759, 2013.

475 Kerminen, V.-M., Paramonov, M., Anttila, T., Riipinen, I., Fountoukis, C., Korhonen, H., Asmi, E., Laakso, L., Lihavainen,  
476 H., Swietlicki, E., Svenningsson, B., Asmi, A., Pandis, S. N., Kulmala, M., and Petäjä, T.: Cloud condensation nuclei  
477 production associated with atmospheric nucleation: a synthesis based on existing literature and new results, *Atmos.  
478 Chem. Phys.*, 12, 12037–12059, 2012.

479 Kulmala, M., Vehkamäki, H., Petäjä, T., Dal Maso, M., Lauri, A., Kerminen, V.-M., Birmili, W., and McMurry, P.:  
480 Formation and growth rates of ultrafine atmospheric particles: a review of observations, *J. Aerosol Sci.*, 35, 143–176,  
481 2004.

482 Kulmala, M., Petäjä, T., Nieminen, T., Sipilä, M., Manninen, H. E., Lehtipalo, K., Dal Maso, M., Aalto, P. P., Junninen, H.,  
483 Paasonen, P., Riipinen, I., Lehtinen, K. E. J., Laaksonen, A., and Kerminen, V.-M.: Measurement of the nucleation of  
484 atmospheric aerosol particles, *Nature Protocols*, 7, 1651–1667, doi:10.1038/nprot.2012.091, 2012.

485 Kulmala, M., Kontkanen, J., Junninen, H., Lehtipalo, K., Manninen, H. E., Nieminen, T., Petäjä, T., Sipilä, M.,  
486 Schobesberger, S., Rantala, P., Franchin, A., Jokinen, T., Järvinen, E., Äijälä, M., Kangasluoma, J., Hakala, J., Aalto,  
487 P.P., Paasonen, P., Mikkilä, J., Vanhanen, J., Aalto, J., Hakola, H., Makkonen, U., Ruuskanen, T., Mauldin, R. L. III,  
488 Duplissy, J., Vehkamäki, H., Bäck, J., Kortelainen, A., Riipinen, I., Kurtén, T., Johnston, M. V., Smith, J. N., Ehn, M.,  
489 Mentel, T. F., Lehtinen, K. E. J., Laaksonen, A., Kerminen, V.-M., and Worsnop, D. R.: Direct observations of  
490 atmospheric aerosol nucleation, *Science*, 339, 943–946, 2013.

491 Makkonen, R., Asmi, A., Kerminen, V.-M., Boy, M., Arneth, A., Hari, P., and Kulmala, M.: Air pollution control and  
492 decreasing new particle formation lead to strong climate warming, *Atmos. Chem. Phys.*, 12, 1515–1524, 2012.

493 Manninen, H. E., Nieminen, T., Asmi, E., Gagné, S., Häkkinen, S., Lehtipalo, K., Aalto, P., Vana, M., Mirme, A., Mirme, S.,  
494 Hörrak, U., Plass-Dülmer, C., Stange, G., Kiss, G., Hoffer, A., Törö, N., Moerman, M., Henzing, B., de Leeuw, G.,  
495 Brinkenberg, M., Kouvarakis, G. N., Bougiatioti, A., Mihalopoulos, N., O'Dowd, C., Ceburnis, D., Arneth, A.,  
496 Svenningsson, B., Swietlicki, E., Tarozzi, L., Decesari, S., Facchini, M. C., Birmili, W., Sonntag, A., Wiedensohler, A.,  
497 Boulon, J., Sellegri, K., Laj, P., Gysel, M., Bukowiecki, N., Weingartner, E., Wehrle, G., Laaksonen, A., Hamed, A.,  
498 Joutsensaari, J., Petäjä, T., Kerminen, V.-M., and Kulmala, M.: EUCAARI ion spectrometer measurements at 12  
499 European sites - analysis of new-particle formation events, *Atmos. Chem. Phys.*, 10, 7907–7927, 2010.

500 Merikanto, J., Spracklen, D. V., Mann, G. W., Pickering, S. J., and Carslaw, K. S.: Impact of nucleation on global CCN,  
501 *Atmos. Chem. Phys.*, 9, 8601–8616, 2009.

502 Morawska, L., Ristovski, Z., Jayaratne, E. R., Keogh, D. U., and Ling, X.: Ambient nano and ultrafine particles from motor  
503 vehicle emissions: characteristics, ambient processing and implications on human exposure, *Atmos. Environ.*, 42, 8113–  
504 8138, 2008.

505 Németh, Z., Rosati, B., Ziková, N., Salma, I., Bozó, L., Dameto de España, C., Schwarz, J., Ždímal, V., and Wonaschütz, A.:  
506 Comparison of atmospheric new particle formation and growth events in three Central European cities, submitted in  
507 2017.

508 Nieminen, T., Kerminen, V.-M., Petäjä, T., Manninen, H. E., Aalto, P. P., Arshinov, M., Asmi, E., Baltensberger, U.,  
509 Beukes, J. P., Collins, D., Harrison, R. M., Henzing, B., Hooda, R., Hu, M., Hörrak, U., Kivekäs, N., Komsaare, K.,  
510 Krejčí, R., Laakso, L., Laaksonen, A., Leaitch, R., Lihavainen, H., Mihalopoulos, N., Németh, Z., O'Dowd, C., Salma, I.,  
511 Sellegri, K., Svenningsson, B., Swietlicki, E., Tunved, P., Ulevicius, V., Vakkari, V., Vana, M., Virtanen, A.,  
512 Wiedensohler, A., and Kulmala, M.: Global analysis of continental boundary layer new particle formation based on long-  
513 term measurements, *Atmos. Chem. Phys. Discuss.*, to be submitted in 2017.

514 Oberdörster, G., Oberdörster, E., and Oberdörster, J.: Nanotoxicology: an emerging discipline evolving from studies of  
515 ultrafine particles, *Environ. Health Perspect.*, 113, 823–839, 2005.

516 OKJ (National register of road vehicles, in Hungarian), 2015. Ministry of National Development, Budapest.

517 Paasonen, P., Kupiainen, K., Klimont, Z., Visschedijk, A., Denier van der Gon, H. A. C., and Amann, M.: Continental  
518 anthropogenic primary particle number emissions, *Atmos. Chem. Phys.*, 16, 6823–6840, 2016.

519 Park, K., Park, J. Y., Kwak, J.-H., Cho, G. N., and Kim, J.-S.: Seasonal and diurnal variations of ultrafine particle  
520 concentration in urban Gwangju, Korea: Observation of ultrafine particle events, *Atmos. Environ.*, 42, 788–799, 2008.

521 Pikridas, M., Sciare, J., Freutel, F., Crumeyrolle, S., von der Weiden-Reinmüller, S.-L., Borbon, A., Schwarzenboeck, A.,  
522 Merkel, M., Crippa, M., Kostenidou, E., Psichoudaki, M., Hildebrandt, L., Engelhart, G. J., Petäjä, T., Prévôt, A. S. H.,  
523 Drewnick, F., Baltensperger, U., Wiedensohler, A., Kulmala, M., Beekmann, M., and Pandis, S. N.: In situ formation and  
524 spatial variability of particle number concentration in a European megacity, *Atmos. Chem. Phys.*, 15, 10219–10237,  
525 2015.

526 Posner, L. N. and Pandis, S. N.: Sources of ultrafine particles in the Eastern United States, *Atmos. Environ.*, 111, 103–112.  
527 2015.

528 Putaud, J.-P., Van Dingenen, R., Alastuey, A., Bauer, H., Birmili, W., Cyrys, J., Flentje, H., Fuzzi, S., Gehrig, R., Hansson,  
529 H. C., Harrison, R. M., Herrmann, H., Hitznerberger, R., Hüglin, C., Jones, A. M., Kasper-Giebl, A., Kiss, G., Koussa, A.,  
530 Kuhlbusch, T. A. J., Löschau, G., Maenhaut, W., Molnár, A., Moreno, T., Pekkanen, J., Perrino, C., Pitz, M., Puxbaum,  
531 H., Querol, X., Rodriguez, S., Salma, I., Schwarz, J., Smolik, J., Schneider, J., Spindler, G., ten Brink, H., Tursic, J.,  
532 Viana, M., Wiedensohler, A., and Raes, F.: A European Aerosol Phenomenology - 3: physical and chemical  
533 characteristics of particulate matter from 60 rural, urban, and kerbside sites across Europe, *Atmos. Environ.*, 44, 1308–  
534 1320, 2010.

535 Reddington, C. L., Carslaw, K. S., Spracklen, D. V., Frontoso, M. G., Collins, L., Merikanto, J., Minikin, A., Hamburger, T.,  
536 Coe, H., Kulmala, M., Aalto, P., Flentje, H., Plass-Dülmer, C., Birmili, W., Wiedensohler, A., Wehner, B., Tuch, T.,  
537 Sonntag, A., O'Dowd, C. D., Jennings, S. G., Dupuy, R., Baltensperger, U., Weingartner, E., Hansson, H.-C., Tunved, P.,  
538 Laj, P., Sellegri, K., Boulon, J., Putaud, J.-P., Gruening, C., Swietlicki, E., Roldin, P., Henzing, J. S., Moerman, M.,  
539 Mihalopoulos, N., Kouvarakis, G., Ždímal, V., Zíková, N., Marinoni, A., Bonasoni, P., and Duchi, R.: Primary versus  
540 secondary contributions to particle number concentrations in the European boundary layer, *Atmos. Chem. Phys.*, 11,  
541 12007–12036, 2011.

542 Rodríguez, S. and Cuevas, E.: The contributions of “minimum primary emissions” and “new particle formation  
543 enhancements” to the particle number concentration in urban air, *J. Aerosol Sci.*, 38, 1207–1219, 2007.

544 Salma, I., Borsós, T., Weidinger, T., Aalto, P., Hussein, T., Dal Maso, M., and Kulmala, M.: Production, growth and  
545 properties of ultrafine atmospheric aerosol particles in an urban environment, *Atmos. Chem. Phys.*, 11, 1339–1353, 2011.

546 Salma, I., Borsós, T., Németh, Z., Weidinger, T., Aalto, P., and Kulmala, M.: Comparative study of ultrafine atmospheric  
547 aerosol within a city, *Atmos. Environ.*, 92, 154–161, 2014.

548 Salma, I., Németh, Z., Weidinger, T., Kovács, B., and Kristóf, G.: Measurement, growth types and shrinkage of newly  
549 formed aerosol particles at an urban research platform, *Atmos. Chem. Phys.*, 16, 7837–7851, 2016a.

550 Salma, I., Németh, Z., Kerminen, V.-M., Aalto, P., Nieminen, T., Weidinger, T., Molnár, Á., Imre, K., and Kulmala, M.:  
551 Regional effect on urban atmospheric nucleation, *Atmos. Chem. Phys.*, 16, 8715–8728, 2016b.

552 Salma, I., Németh, Z., Weidinger, T., Maenhaut, W., Claeys, M., Molnár, M., Major, I., Ajtai, T., Utry, N., and Bozóki, Z.:  
553 Source apportionment of carbonaceous chemical species to fossil fuel combustion, biomass burning and biogenic  
554 emissions by a coupled radiocarbon–levoglucosan marker method, *Atmos. Chem. Phys.*, 17, 13767–13781, 2017.

555 Samoli, E., Andersen, Z. J., Katsouyanni, K., Hennig, F., Kuhlbusch, T. A. J., Bellander, T., Cattani, G., Cyrus, J.,  
556 Forastiere, F., Jacquemin, B., Kulmala, M., Lanki, T., Loft, S., Massling, A., Tobias, A., and Stafoggia, M.: Exposure to  
557 ultrafine particles and respiratory hospitalisations in five European cities, *Eur. Resp. J.*, 48, 674–682, 2016.

558 Shen, L., Mickley, L. J., and Murray, L. T.: Influence of 2000–2050 climate change on particulate matter in the United  
559 States: results from a new statistical model, *Atmos. Chem. Phys.*, 17, 4355–4367, 2017.

560 Shi, J. P., Khan, A. A., and Harrison, R. M.: Measurements of ultrafine particle concentration and size distribution in the  
561 urban atmosphere, *Sci. Total Environ.*, 235, 51–64, 1999.

562 Spracklen, D. V., Carslaw, K. S., Kulmala, M., Kerminen, V.-M., Mann, G. W., and Sihto, S.-L.: The contribution of  
563 boundary layer nucleation events to total particle concentrations on regional and global scales, *Atmos. Chem. Phys.*, 6,  
564 5631–5648, 2006.

565 Spracklen, D. V., Carslaw, K. S., Kulmala, M., Kerminen, V.-M., Sihto, S.-L., Riipinen, I., Merikanto, J., Mann, G. W.,  
566 Chipperfield, M. P., Wiedensohler, A., Birmili, W., and Lihavainen, H.: Contribution of particle formation to global  
567 cloud condensation nuclei concentrations, *Geophys. Res. Lett.*, 35, L06808, doi:10.1029/2007GL033038, 2008.

568 Wiedensohler, A., Birmili, W., Nowak, A., Sonntag, A., Weinhold, K., Merkel, M., Wehner, B., Tuch, T., Pfeifer, S., Fiebig,  
569 M., Fjåraa, A.M., Asmi, E., Sellegri, K., Depuy, R., Venzac, H., Villani, P., Laj, P., Aalto, P., Ogren, J.A., Swietlicki, E.,  
570 Williams, P., Roldin, P., Quincey, P., Hüglin, C., Fierz-Schmidhauser, R., Gysel, M., Weingartner, E., Riccobono, F.,  
571 Santos, S., Gröning, C., Faloon, K., Beddows, D., Harrison, R., Monahan, C., Jennings, S. G., O’Dowd, C. D., Marinoni,  
572 A., Horn, H.-G., Keck, L., Jiang, J., Scheckman, J., McMurry, P. H., Deng, Z., Zhao, C. S., Moerman, M., Henzing, B.,  
573 de Leeuw, G., Löschau, G., and Bastian, S.: Mobility particle size spectrometers: harmonization of technical standards  
574 and data structure to facilitate high quality long-term observations of atmospheric particle number size distributions,  
575 *Atmos. Meas. Tech.*, 5, 657–685, 2012.

576 Xiao, S., Wang, M. Y., Yao, L., Kulmala, M., Zhou, B., Yang, X., Chen, J. M., Wang, D. F., Fu, Q. Y., Worsnop, D. R., and  
577 Wang, L.: Strong atmospheric new particle formation in winter in urban Shanghai, China, *Atmos. Chem. Phys.*, 15,  
578 1769–1781, 2015.

579 Yu, F., Luo, G., Pryor, S. C., Pillai, P. R., Lee, S. H., Ortega, J., Schwab, J. J., Hallar, A. G., Leaitch, W. R., Aneja, V. P.,  
580 Smith, J. N., Walker, J. T., Hogrefe, O., and Demerjian, K. L.: Spring and summer contrast in new particle formation  
581 over nine forest areas in North America, *Atmos. Chem. Phys.*, 15, 13993–14003, 2015.